Journal of Physics:
Conference Series

PAPER • OPEN ACCESS

Numerical investigation of fill height and secondary currents in an inclined partially filled pipe flow

To cite this article: Aniruddha Bose *et al* 2024 *J. Phys.: Conf. Ser.* **2899** 012017

Journal of Physics: Conference Series **2899** (2024) 012017
doi:10.1088/1742-6596/2899/1/012017

Numerical investigation of fill height and secondary currents in an inclined partially filled pipe flow

Aniruddha Bose[1*], Duncan J Borman[2], Timothy N Hunter[3], Julian T Spencer[4] and Christopher J Cunliffe[5]

[1] School of Computing, University of Leeds, Woodhouse Lane, Leeds, LS2 9JT, UK
[2] School of Civil Engineering, University of Leeds, Woodhouse Lane, Leeds, LS2 9JT, UK
[3] School of Chemical and Process Engineering, University of Leeds, Woodhouse Lane, Leeds, LS2 9JT, UK
[4] National Nuclear Laboratory, Chadwick House, Birchwood Business Park, Warrington, Cheshire, WA3 6AE, UK
[5] National Nuclear Laboratory, Havelock Rd, Workington, Cumbria, CA14 3YQ, UK

*E-mail: scabo@leeds.ac.uk

Abstract. Partially filled pipes are used in industrial processes to transport liquid and particle laden flows. A good understanding of the three-dimensional flow in these pipes is critical to ensure material is transported without issue, for example without particulates settling out. In this work, air-water two-phase flows in a partially filled pipe geometry of an industrial slurry transport rig are investigated using unsteady Volume of Fluid (VOF) RANS model in OpenFOAM to investigate fill height and secondary currents. Both are important factors in partially filled pipes where the water depth and secondary current strength can influence solid particle transport and settling. The study confirms that the CFD approach can reliably predict the flow depth across a range of pipe inclination and the secondary currents are predicted in good qualitative agreement with those seen in other studies. The effect of pipe inclination on fill height and the effect of fill height on secondary currents are investigated for a range of mass flow rates. The results of fill height agree well with the experiments and are in line with the Manning equation for a hydraulically smooth pipe. Secondary current strength is seen to increase with fill height in agreement with other studies.

1. Introduction

Partially filled pipe flows are common in several industrial applications where water or other liquids are transported from one place to another, often with suspended solid particles. Examples include petrochemical, food processing, mining, and sewerage systems where slurry flows are typically either driven by pressure gradient or gravity [1], [2]. Studies investigating gravity-driven partially filled pipe flows are infrequent in the literature when compared to pressure-driven flows. A lot of industrial settings employ gravity-driven flows and therefore there is an interest in understanding the mechanisms going on inside such a system and our ability to reliably predict these with computational models. Flow in a gravity-driven partially filled pipe can be described by the Manning equation [3]

$$U_b = \frac{1}{n} R_h^{2/3} \sqrt{S} \quad (1)$$

where U_b is the bulk velocity of the flow, R_h is the hydraulic radius [3], which is given by the ratio of the flow cross-sectional area to the wetted perimeter, and S is the channel slope. The empirical coefficient n is the Manning roughness coefficient and is taken as 0.009 for hydraulically smooth pipes [3].

Partially filled pipe flows are different from fully filled pipes because of the presence of secondary currents [1]. Secondary currents are induced at the corners of the air-water interface inside the pipe due to the presence of the air-phase and non-circular fluid cross-sectional area (an example from simulations shown in Figure 5). These secondary currents occur in the plane of the cross-section of the liquid inside the pipe and change the dynamics of the system, particularly, the velocity field and pressure gradient [1]. Therefore, it is important that models accurately predict these secondary currents.

Previous studies of flow inside a partially filled pipe have focused on rapid filling in pipeline systems and the associated air-water interaction and interface evolution through both experimental and computational studies [4-7], CFD and experimental studies of the movement of an entrapped air pocket during pipe filling and its effect on pressure surges [2], [8-11], and numerical modelling of geyser or explosive eruptions of air and water due to release of entrapped air pocket [12]. Experimental studies have focused on investigation of heat transfer [13] and continuous single-phase rimming flow [14] in a rotating, partially filled pipe. Additionally, CFD studies have investigated shear stress distribution [15] and the effect of bed roughness on velocity distribution and shear stress [16] in partially filled pipes. The authors in [1] computationally investigated the effect of secondary currents on friction factor and turbulent structures in partially filled pipes. They showed that secondary currents are more dominant for half-filled and three quarter filled pipes as compared to quarter filled pipes. In [17], the authors have performed experiments on partially filled laminar and turbulent pipe flows and showed that the presence of secondary currents heavily distorts the mean streamwise velocity distribution in turbulent flows.

Despite the notable research, there are few studies investigating the effect of pipe inclination on water depth and the impact of water depth on secondary currents in partially filled pipes. Both these flow characteristics are important in cases where partially filled pipes transport solid particles as both the depth of the water (and the associated secondary currents) influence solid particle transport and settling.

Thus, the aim of this study is to computationally investigate the effect of pipe inclination on fill height (d) inside a partially filled pipe, and the effect of fill height on secondary currents acting on the cross-section of the pipe and compare to other studies.

2. Flow Description and Numerical Modelling

2.1 CFD setup and Methodology

The pipe geometry used in this study is based on the experimental slurry transport rig used in [3]. To the best of the authors' knowledge, a CFD study on the same geometry has not been performed before. Two pipes, each of length 12 m and diameters, D_1 = 0.0763 m (marked D in Figure 1a), and D_2 = 0.1 m (marked E in Figure 1a) are used in the experimental studies. The angle of inclination of the pipe of diameter D_1 is 1 % and that of the other is 5 %. Water or slurry enters the working section of the pipe from a header tank (marked B in Figure 1a) via a short vertical drop. There is a flow meter shortly after the drop (early in the inclined working section) that also acts to stabilise the flow. There is a small opening to the atmosphere in the roof of the pipe to allow air to be drawn in (located shortly after the flow meter). Figure 1 shows a photograph of the experimental rig alongside a representation of the 5-metre-long modelling domain considered in this study. Further details of the experimental setup can be found in [3].

The CFD model uses a simplified configuration by removing the header tank and the initial vertical drop and replacing with an equivalent representative boundary condition. This is done after conducting a sensitivity study, where same results were obtained downstream of the pipe irrespective of whether the initial vertical drop is simulated or not. Tests were conducted on both 12 m and 5 m pipe lengths and they both yielded comparable downstream results. Therefore, to save computational time, the CFD results are given for a 5 m pipe length for both D_1 and D_2. At the model inlet, a small area covering about 25 % of the total area is provided for air entry, and the

a)

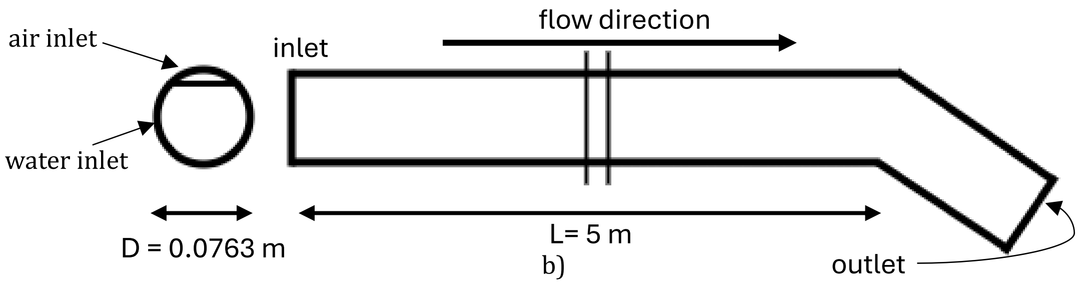

b)

Figure 1. Experimental photo and CFD setup: a) photo of the experimental setup [3] used as a basis for CFD studies, b) schematic of the CFD model showing boundary conditions (not to scale).

rest is water. This is done to stabilise the flow inside the pipe and replicate the experimental conditions. At the outlet, backflow of water is prevented and a no-slip condition is imposed on the walls. A break is shown by parallel lines on the model pipe to represent the entire length in the space available.

A 3D hexahedral mesh for the pipe geometry is used. The isometric and the cross-sectional view of the mesh are shown in Figure 2. After a mesh independence study, the optimum number of mesh elements was found to be 1.7M. The simulations were performed at mass flow rates ranging from 0.2778 kg/s to 2.083 kg/s which is equivalent to hydraulic Reynolds number (Re_h) (as in [3]) of 1.519×10^4 to 6.863×10^4. For pipe diameter, D_1 = 0.0763 m, four different slopes of 1 %, 2 %, 3 % and 5 % and for D_2 = 0.1 m, three different slopes of 3 %, 5 % and 7 % are simulated.

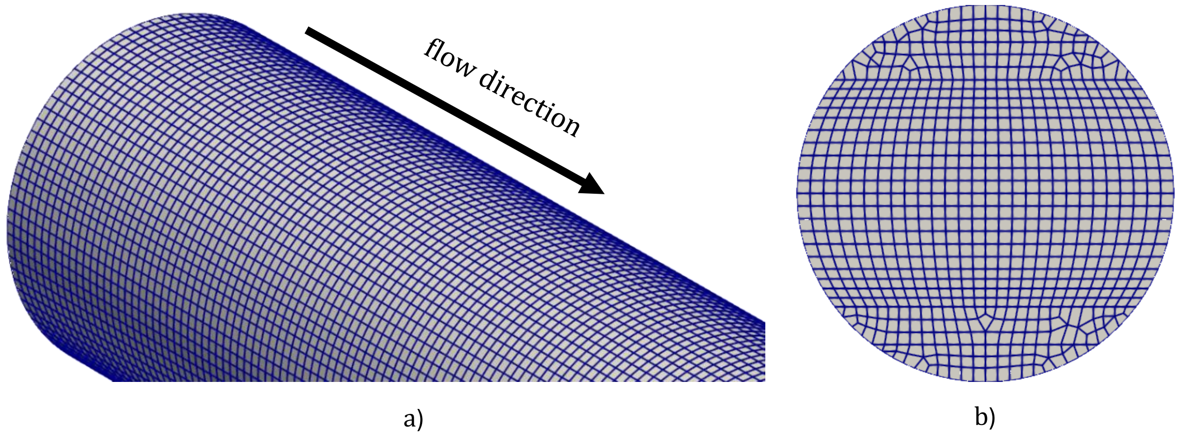

Figure 2. Mesh, a) hexahedral mesh on a part of the pipe along the length, b) mesh on the inlet cross-section of the pipe

2.2 Governing equations and numerical methods

The multiphase solver interFoam within the CFD software suit OpenFOAM is used to conduct unsteady two-phase air-water simulations by solving the Reynolds Averaged Navier Stokes (RANS) equations utilising the the k-ε RNG turbulence model. The solver solves for two incompressible, isothermal and immiscible fluids (i.e. water and air in this case) using the continuity and momentum equation alongise using a transport equation to calculate the water volume fraction using a Volume of Fluid (VOF) approach. The MULES interface capturing scheme is implemented. Finite volume method is used and the solution is undertaken by PIMPLE algorithm which is a combination of PISO and SIMPLE. The details of the equations can be found in [18].

3. Results and discussion

The streamwise component of the flow reaches a steady state at around 14 seconds after the flow is started. Flow measurements were taken at 4 meters downstream of the pipe to ensure a fully developed flow. Figure 3 shows different features of the flow for pipe slope = 1 % and mass flow rate = 1.8 kg/s. Figure 3a) shows the variation of the free surface position of the flow with time represented by fill height ratio (d/D) vs time. It is seen that at around 14 seconds, the free surface position stops changing with time and becomes horizontal. This is indicated by a dashed horizontal line in Figure 3a) and has a value, d/D = 46.06 %. Figure 3b) shows the water-free surface and fill height on a 2D plane for b1) an initial 0.2 m from the inlet and b2) between 3.5 m and 4.1 m of the pipe once the flow has reached a steady state. Fill height reaches a constant value along the length of the pipe. Figure 3c) shows the water-free surface as a 3D iso-surface coloured by the velocity magnitude between 3.5 m and 4.1 m of the pipe.

3.1 Calculation of fill height and comparison to experiments

To calculate the fill height ratio (d/D), the position of the water free surface is measured perpendicular to the pipe length at 4 m downstream of the pipe inlet which corresponds to a water volume fraction value = 0.5. The hydraulic Reynolds number (Re_h) associated with a partially filled pipe flow is calculated as per [3]. This operation is repeated for each combination of mass flow rates, pipe slope and pipe diameter. The Manning equation corresponding to fill

Journal of Physics: Conference Series **2899** (2024) 012017
doi:10.1088/1742-6596/2899/1/012017

height ratio (d/D) vs. Re_h is obtained by modifying the original Manning equation (1) based on [3].

CFD results for d/D vs. Re_h are plotted for each slope along with experimental data [3] and the modified Manning equation for fill height in Figure 4. Figures 4 a) and b) respectively show the graph of fill height (d/D) vs. Re_h for pipe diameters, D_1 = 0.0763 m, and D_2 = 0.1 m. It is seen that the CFD data is in good agreement but slightly underpredicts the Manning equation and the experimental data. Therefore, it is surmised that the CFD model results predict for a marginally smoother pipe than predicted by the Manning equation with a value of n = 0.009. It is also seen that for higher slopes the fill height reduces for the same mass flow rate as expected.

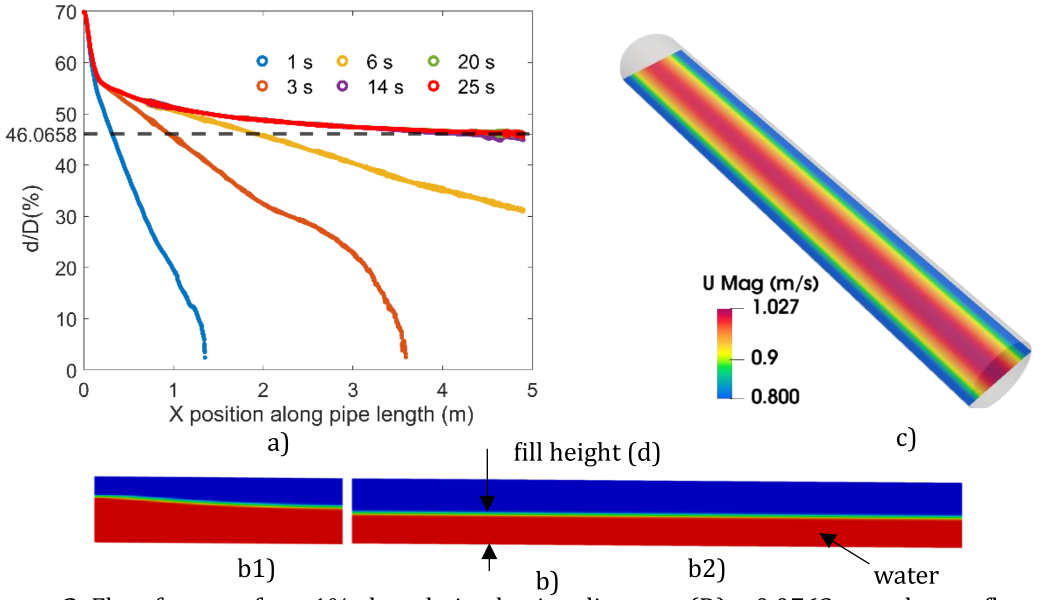

Figure 3. Flow features for a 1% sloped pipe having diameter (D) = 0.0763 m and mass flow rate = 1.8 kg/s, a) variation of water free surface position with time after flow commences, b) water free surface showing the fill height at 15 s on a 2D mid plane along pipe length between b1) 0 – 0.2 m and b2) 3.5 m – 4.1 m , c) 3D iso water free surface coloured by velocity magnitude at 15 s between pipe length 3.5 m and 4.1 m

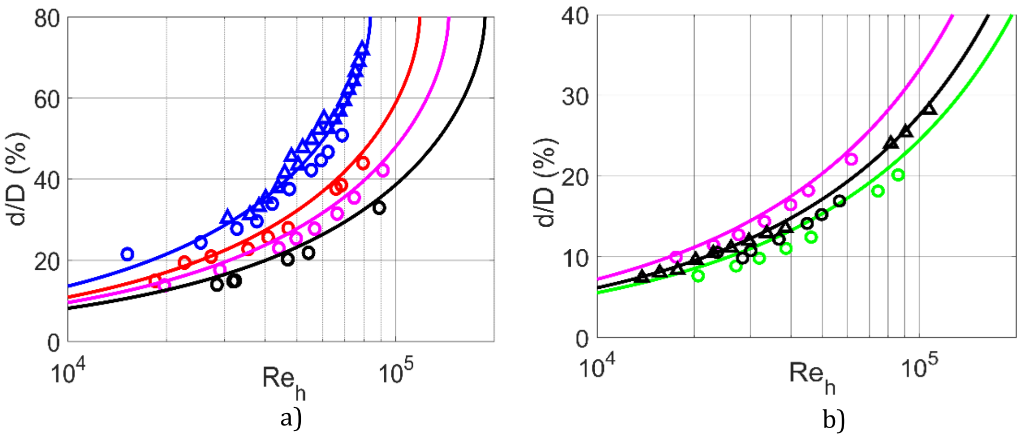

Figure 4. Comparison of fill height ratio vs. Re_h between CFD, experimental values [3] and the Manning equation [3]: a) pipe diameter = 0.0763 m, b) pipe diameter = 0.1 m, solid lines represent Manning equation [3], circles represent CFD values at 4 m, triangles represent experimental values [3]. (Pipe slope: blue = 1 %, red = 2 %, pink = 3%, black = 5 %, green = 7 %)

3.2 Secondary currents and relation with fill height

After verifying that the CFD model was in appropriate agreement with the experimental data and the respective Manning equation predictions, the secondary currents are explored, along with the effect of the fill height on secondary current strength. As mentioned, secondary currents originate due to the presence of the air-water interface and are very important as they influence the mean streamwise velocity in partially filled pipes [1]. For sloped pipes, the cross section is taken perpendicular to the pipe length to correctly visualise the secondary currents.

The strength of the secondary flow is given by

$$U_s = \sqrt{v^2 + w^2} \tag{2}$$

for a steady flow, where v *and* w are the y and z component of the flow on a cross section of the pipe. Figure 5 shows the contour plot of secondary current strength for four different fill heights (obtained by changing the mass flow rate) for pipe diameter, D_1 = 0.0763 m and slope = 1 % obtained from CFD simulations at 4 m downstream of the pipe and at 25 s.

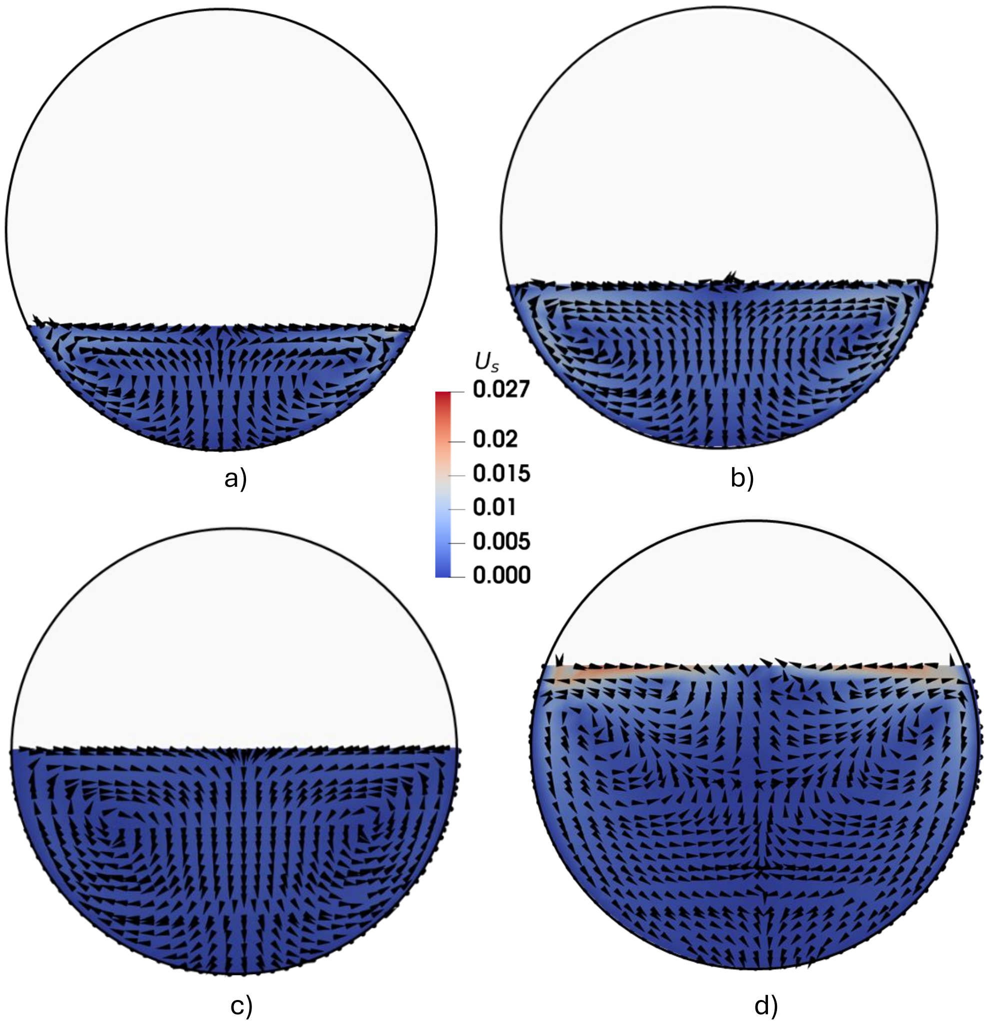

Figure 5. Secondary current strength contours at different fill height ratio (d/D): a) d/D = 27 %, b) d/D = 37.57 %, c) d/D = 50 % and d) d/D = 63.3 %. The secondary vectors are superimposed on the contour

The contour plots are superimposed with secondary vectors which show the rotating phenomenon. The secondary currents are seen to increase from the bottom of the cross section, moving close to the pipe wall towards the free surface with maximum values near the free surface, before the flow descends close to the middle.

A pair of symmetric vortices are seen for each case which is consistent with [1], [17]. Next, the averaged secondary current strength (U_{sb}) is calculated for each fill height for the above pipe by averaging the cell data on the entire cross section covered by water at pipe downstream location of 4 m. It is seen that U_{sb} increases with fill height because the secondary flow has more space to develop in higher water depth. The percentage increase in U_{sb} from a fill height of 25 % to 50 % is about 50 %. The averaged secondary strength for a quarter filled pipe flow is found to be about 1.13 % of the bulk velocity. Flows with other fill heights also show similar ranges. All these findings are in close agreement with [1], who reported that the secondary current strength for a quarter filled pipe does not exceed 1.5 % of the bulk velocity.

A scatter plot showing the cross-sectional averaged secondary flow strength (U_{sb}) vs. fill height ratio (d/D) (%) in blue circles and ratio of U_{sb} and bulk velocity (U_b) vs d/D (%) in red circles is shown in Figure 6 for pipe diameter = 0.0763 m and slope = 1 % and at 25 s. A dashed line is drawn along the CFD values represented by circles for visual aid. It can be seen that U_{sb} increases with fill height as explained before, but the ratio U_{sb}/U_b shows small variation and is almost constant.

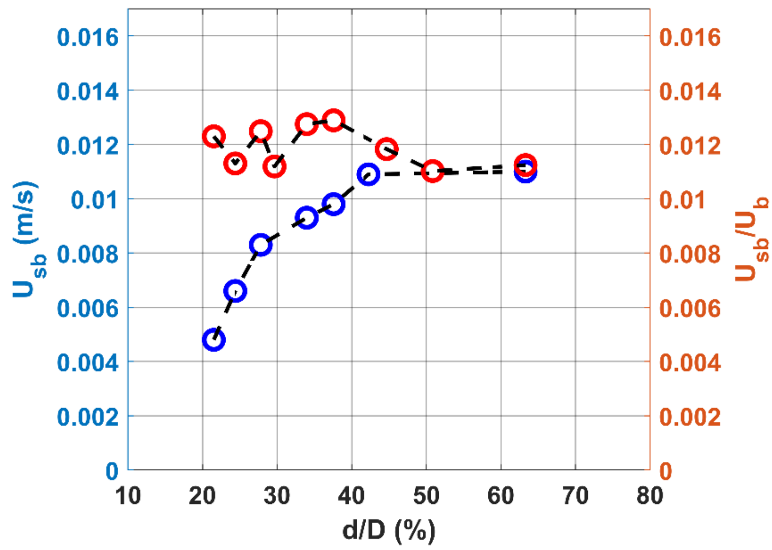

Figure 6. CFD predictions showing U_{sb} (m/s) vs. d/D (%) (blue circles) and U_{sb}/U_b vs. d/D (%) (red circles). Dashed lines are connecting the circles and are shown for visual aid

Thus, the ratio of the averaged secondary current strength to the bulk velocity for the 1 % sloped pipe is near the value of 0.012 for different fill heights. This is because with increasing fill height (which is obtained by increasing mass flow rate), bulk velocity and secondary flow both increases.

4. Conclusion

In this study, fill height ratio and secondary currents are explored in a partially filled pipe flow through CFD simulations. The effect of pipe inclination on fill height is shown and compared to experimental values and the Manning equation. Close agreement is reached between CFD and experiments. It is seen that fill height reduces with pipe inclination.

Secondary currents are observed on the pipe cross-section and is seen to increase in strength with fill height ratio. Contour plots of secondary current strengths are plotted at different water depth and are compared to other literature. Good agreement of secondary strength values is found between this study and existing literature. It is concluded that secondary current strength increases with fill height or water depth and the ratio of averaged secondary current strength to bulk velocity is almost constant for the 1 % inclined pipe. All these findings will be helpful in analysing our next research question, where solid particle transportation and deposition will be studied in a partially filled pipe flow and how the in-plane water motion affects the movement of the particles.

5. Acknowledgement

The authors gratefully acknowledge the help received from the High-performance computing facilities of the University of Leeds, and guidance and funding received from Sellafield Ltd, UK and National Nuclear Laboratory, UK.

6. References

[1] Liu Y, Stoesser T and Fang H 2022 *J. Fluid Mech.* **938** A16
[2] Zhou L, Liu D and Ou C 2011 *Eng. Appl. Comput. Fluid Mech.* **5** 127-140
[3] Cunliffe C J, Dodds J M and Dennis D J C 2021 *Chem. Eng. Sci*. **235** 116465
[4] Hou Q et al. 2014 *J. Hydraul. Eng.* **140** 04014053
[5] Vasconcelos J G and Wright S J 2008 *J. Hydraul. Eng.* **134** 984-992
[6] Trindade B C and Vasconcelos J G 2013 *J. Hydraul. Eng.* **139** 921-934
[7] Wang H and Chanson H 2015 *Urban Water J.* **12** 502-518
[8] Paternina-Verona DA, Coronado-Hernandez OE, Espinoza-Roman H G, Fuertes-Miquel V S and Ramos H M 2023 *Water* **15** 834
[9] Zhou L, Wang H, Karney B, Liu D, Wang P and Guo S 2018 *J. Hydraul. Eng.* **144** 04018045
[10] Huang B, Fan M, Liu J and Zhu D Z, 2021 *World Environmental and Water Resources Congress* 495-507
[11] Zhou L and Liu D 2013 *J. Hydraul. Res.* **51** 469-474
[12] Chan S N, Cong J and Lee J H W 2018 *J. Hydraul. Eng.***144** 04017071
[13] Chatterjee S, Sugilal G and Prabhu S V 2018 *Int. J. Therm. Sci.* **125** 132-141
[14] Singaram S S, Lodha H and Jachuck R J 2014 *AIChE Journal* **60** 3939-3950
[15] Berlamont J E, Trouw K and Luyckx G 2003 *J. Hydraul. Eng.* **129** 697-705
[16] Alihosseini M and Thamsen P U 2019 *Technische Mechanik-European Journal of Engineering Mechanics* **39** 113-124
[17] Ng H C-H, Cregan H L F, Dodds J M, Poole R J and Dennis D J C 2018 *J. Fluid Mech.* **848** 467-507
[18] OpenCFD Ltd. OpenFOAM version 7 September 2, 2019 https://doc.cfd.direct/openfoam/user-guide-v7/index